

PAPER • OPEN ACCESS

## Impact Assessment of Breaking Waves Criteria Subjected to Wave Energy Converter

To cite this article: Rudi Walujo Prastianto *et al* 2022 *IOP Conf. Ser.: Earth Environ. Sci.* **1081** 012049

View the [article online](#) for updates and enhancements.

You may also like

- [Tidal Wave Breaking in the Eccentric Lead-in to Mass Transfer and Common Envelope Phases](#)  
Morgan MacLeod, Michelle Vick and Abraham Loeb
- [Scanning the parameter space of collapsing rotating thin shells](#)  
Jorge V Rocha and Raphael Santarelli
- [Closed timelike curves and 'effective' superluminal travel with naked line singularities](#)  
Caroline Mallary, Gaurav Khanna and Richard H Price



The Electrochemical Society  
Advancing solid state & electrochemical science & technology

**242nd ECS Meeting**  
Oct 9 – 13, 2022 • Atlanta, GA, US  
Presenting more than 2,400 technical abstracts in 50 symposia

**ECS Plenary Lecture**  
featuring  
**M. Stanley Whittingham**,  
Binghamton University  
Nobel Laureate –  
2019 Nobel Prize in Chemistry

Register now!

The advertisement features the ECS logo, a portrait of M. Stanley Whittingham with his Nobel Prize medal, and a background image of a person interacting with a futuristic interface of glowing icons.

# Impact Assessment of Breaking Waves Criteria Subjected to Wave Energy Converter

Rudi Walujo Prastianto<sup>1</sup>, Fuad Mahfud Assidiq<sup>2</sup>, and Mukhtasor<sup>1</sup>

<sup>1</sup> Department of Ocean Engineering, Institut Teknologi Sepuluh Nopember, Sukolilo, Surabaya, Indonesia

<sup>2</sup> Department of Ocean Engineering, Universitas Hasanuddin, Bontomarannu, Gowa, Indonesia

E-mail: assidiqfm@unhas.ac.id

**Abstract.** Breaking wave effect on Wave Energy Converter (WEC) represents an important issue of site selection analysis especially fringing reefs area. To learn a more acceptable sense of the influence of this effect, an introspection on the estimate of initial breaker points is proposed in the present study. The paper describes an investigation of the impact assessment of wave-breaking criteria subjected to WEC recently desired as a benchmark by the previous three wave-breaking methods. The numerical simulation is carried out by the Computational Fluid Dynamics (CFD) solver. The solver is based on the Finite Volume Method (FVM) to create the discretization of the governing equations. Large Eddy Simulation (LES) is solved in a global approach together with Volume of Fluid (VoF) for capturing free surface. Reported justifications are compared with the experimental data to validate the accuracy of the numerical approach and then applied to generate wave-breaker point location on a fringing reef in Numerical Wave Tank-based (NWT) of 16 scenarios. The results are discussed with respect to relative wave-breaker locations, relative wave-breaker height range, and wave breaking probability under various wave steepness, water depth, and slope fringing reef. It is given regarding the discrepancy between different methods and recommendations for important guidances are outlined.

## 1. Introduction

Breaking waves are one of the most complicated hydrodynamic models in a coastal area [1]. In terms of nearshore region such as reef dimensions, reef roughness environmental loads, wave run-up, and sediment transport are governed by local hydrodynamic phenomena specifications. Understanding breaking wave generation across the reef is critical not only for extremely low water depths, but also for the impact of wave-reef interaction. Breaking waves in some theoretical schemes are applied to providing a specific description of shallow-water wave nonlinearity, the eddy viscosity, and the macroscopic dissipation [2]. It is also useful for modeling the propagation of long-period waves in shallow water depth [3].

Describing in nonlinear effects [2], breaking wave characteristics together with wave run-up in the reef zone [4], wave-structure interaction and reef current celerity distribution [5], and effects of reef morphology configurations [6] are some of the studies for modeling wave dynamics over reefs. Following that, a numerical wave tank (NWT) was developed, capable of simulating breaking wave and, in many cases, replacing a physical wave tank. Another study focuses on using this



computationally wave breaking method, which includes air entrainment [7], wave breaking on a sloping beach [8], solitary wave run-up process [9], and a hybrid computational scheme of breaking wave dynamics model at specific locations [10].

Furthermore, complex surf zone geometries, surf zone energy dissipations, and nearshore breaking wave have all been supported by smoothed particle hydrodynamics (SPH) [11]. Despite the fact that SPH has become a common technique for ocean engineering problems, its performance in terms of boundary conditions and model convergence is still being improved [12]. Newly developed Boussinesq equations, on the other hand, are better suited to simulating breaking waves on complex reef morphology variations [13]. Even Boussinesq equations are the universal tool due to their computational efficiency, there are still a few drawbacks, such as wave breaking not being well captured and the inability to resolve breaking wave vertical flow due to polynomial approximation. The study generates NWT based on Large Eddy Simulation (LES) to improve the issues of simulating the solitary breaking wave over the reefs using Boussinesq. The LES model may be able to explain significant large-scale unsteadiness flow in greater detail [14]. Because the solitary wave transformation over a reef has been extensively studied in the past, the wave-reef interaction analysis is expected to encourage ocean engineering problems [2].

Yasuda et al. [5] provided experimental and numerical knowledge of breaking solitary waves over flat reef. Particle image velocimetry (PIV) was used to measure free-surface capturing and velocity distribution in various locations. It also used the fully nonlinear boundary integral method (BIM) to numerically model the wave model. Regardless of the fact that the aforementioned studies described intriguing findings, this paper was only given a preliminary examination. The Navier-Stokes equations collaboration between the Volume of Fluid (VoF) terms for free-surface monitoring [15] and LES for turbulence approach [14] is computed by the 3-D NWT. In contrast to a previous study [16], this one focuses on the evaluation of breaking wave criteria when subjected to a wave energy converter under varying tidal conditions.

## 2. Numerical Modelling

The high-level schemes for spatial and temporal discretization approach of the three-dimensional wave breaking criteria subject to wave energy converter installation is carried out using computational fluid dynamic (CFD). The model solves the two-phase fluid turbulent flow problem using large eddy simulation (LES) in a finite volume framework [14,17,18]. The volume of fluid (VoF) is purposed to realize the interface air and water accurately based on split lagrangian scheme. Furthermore, pressure modelling solution is obtained from the generalized minimal residual method (GMRES) which clicks on the convergence rapidly, efficient, and recommended for all flow modelling types [18,19].

The numerical wave tank (NWT) is 22.95 long, 0.55 m wide, and 0.60 high to emulate the wave tank used in the experiments. See previous study [16] for detailed laboratory settings. The dynamic boundary method (DBM) for wave generation is used, with a TMA spectrum scheme [20,21,22,23]. The breaking waves are absorbed at the outlet of NWT using a numerical beach method [24]. The detailed implementation of boundary condition can be followed in the previous work [25,26,14] and Figure 3(c) in the section 3.1. Furthermore, courant frederick lewis (CFL), automatically adjusted on 0.50, is adopted to resolve and emphasize the time steps of 0.01 automatically during 200 wave propagation simulations. Structured mesh is applied to discretize the computational domain, For the whole directions, the mesh size is initially set to be  $\Delta x = \Delta y = \Delta z = 0.03$  m across the domain as illustrated in Figure 1(a). Meanwhile, mesh refinement is constructed circumstantially in the free surface, slope reef, and flat reef zone which are presented in Figure 1(b–c–d), respectively. The total computational mesh consists of 275400 cells. The simulation duration is not appointed to be 40 initially to guarantee the significant transient effect of breaking wave height and mean water depth. Over 8 processors data processing, it takes approximately 10 to 36 hours per simulation on a bundle server with Intel Core I7 7700HQ CPU - 2.80GHz. To assess the performance of the numerical simulation, the common coefficient of determination  $R^2$ , the model Skill value, and mean absolute

percentage error (MAPE) are adopted and calculated by [27,28] as mentioned in equation (1) and (2), respectively.

For LES modelling breaking waves over fringing reef, it is crucial to examine the breaking wave criteria methods at the incipient of breaker point where strong turbulence is created. It could be calculated by equation (3) and (4) concerning locations of relative breaking wave height, equation (5) as the estimation ranges of relative breaking wave heights, and equation (6) and (7) for probability of breaking waves. The detailed description of those can be established in [29,30,31]. Ultimately, the three criteria are considered here to cover most of the existing breaking wave detection methods possibly and related to each other.

$$skill = 1 - \frac{\sum |Y_{num} - Y_{exp}|^2}{\sum (|Y_{num} - \bar{Y}_{exp}| + |Y_{exp} - \bar{Y}_{exp}|)^2} \quad (1)$$

$$MAPE = \frac{\sum \left| \frac{Y_{exp} - Y_{num}}{Y_{exp}} \right|}{n} \times 100 \quad (2)$$

$$\left( \frac{H}{h} \right)_b = \frac{A \left\{ 1 - \exp \left[ -1.5\pi \frac{h_b}{L_0} (1 + B \tan^{4/3} \theta) \right] \right\}}{h_b / L_0} \quad (3)$$

$$\left( \frac{H}{h} \right)_b = \left( \frac{H}{h} \right)_{cr} + \left( \frac{h_b}{L_0} \right)^{-1.023} \times \left\{ \frac{H_0}{L_0} - \left[ 0.410 \times \frac{h_b}{L_0} + 0.950 \times \left( \frac{h_b}{L_0} \right)^2 \right] \right\} \quad (4)$$

$$\left( \frac{H}{h} \right)_b = C \frac{L_0}{h_b} \left\{ 1 - \exp \left[ -1.5\pi \frac{h_b}{L_0} (1 + 11s^{4/3}) \right] \right\} \quad (5)$$

$$F_{br} = \exp \left[ -9.1733 \times 10^{-4} \left( \frac{\alpha}{\varepsilon_s} \right)^2 \right] \quad (6)$$

$$\varepsilon_s = \frac{H_s}{gT_p^2} \quad (7)$$

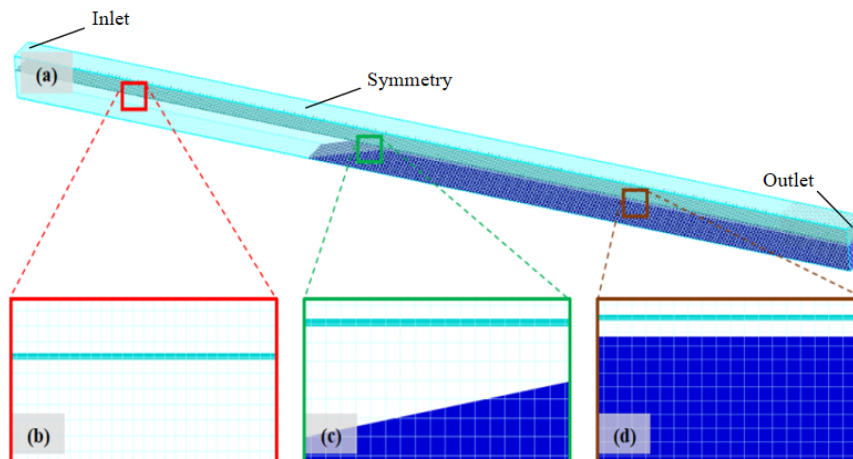


**Figure 1.** The structured meshes and boundary conditions of numerical wave tank (NWT)

### 3. Results and Discussion

The results and discussion of the CFD study are presented in this section. In order to the breaking wave modelling is implemented in real conditions, Spermonde islands, one of Indonesian role model located in South Sulawesi, are adopted in this study which correspond to the fringing reef configuration of [16] as illustrated in Figure 2. The recording for 30 years of sea states of Spermonde, the details are listed in Table 1, is carried out to simulate it by varying water depth  $h$  which represented tidal conditions as shown in Table 2 [32]. To compose easier several scenarios, the code practice is applied such as *A-1* which means the wave parameter  $H_s=0.321$  m,  $T_p=5.791$  s establish in  $h=0.364$  m, etc. Therefore, 16 scenarios of code practice are being simulated that is to say *A-1, B-1, C-1, D-1, A-2, B-2, C-2, D-2, A-3, B-3, C-3, D-3, A-4, B-4, C-4, and D-4*. Besides that, the Froude number and Reynold number scaling are set up based on [33,34].

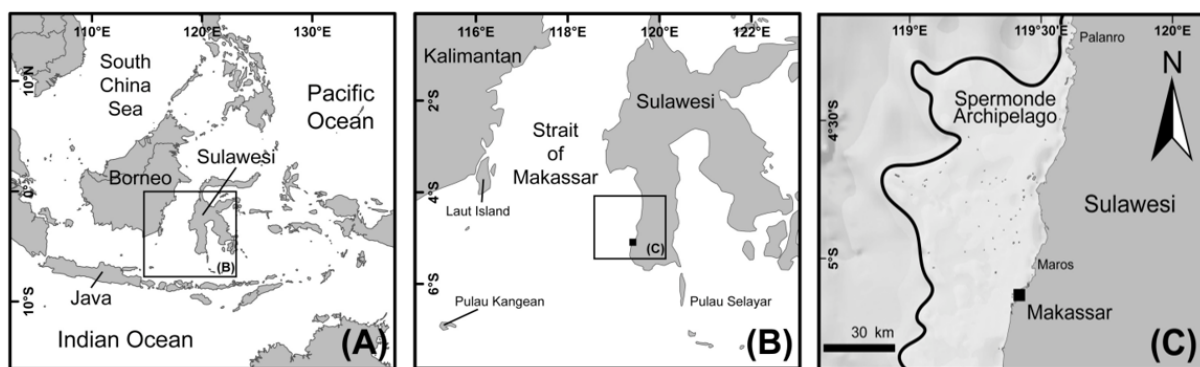


Figure 2. Spermonde islands, the role model of this assessment study

Table 1. Sea states parameter of Spermonde islands

Codes	Existing			Conversion		
	$H_s$ [m]	$T_p$ [s]	Scale Factor	$H_s$ [m]	Scale Factor	$T_p$ [s]
A	0.321	5.791	$\lambda$	0.013	$\lambda^{1/2}$	1.158
B	0.607	4.784	$\lambda$	0.024	$\lambda^{1/2}$	0.957
C	0.750	5.036	$\lambda$	0.030	$\lambda^{1/2}$	1.007
D	1.000	4.532	$\lambda$	0.040	$\lambda^{1/2}$	0.906

Table 2. Parameter of various water depths  $h$

Codes	$h_r$ [m]	$h$ [m]
1	0.014	0.364
2	0.028	0.378
3	0.042	0.392
4	0.056	0.406

#### 3.1. Validation of Numerical Model

Figure 3 compares the numerical and the experimental cross-fringing reef distribution of the free-surface elevations on, where cross-fringing reef distribution, on the parallel view, is correlated with significant wave heights  $H_s$ , mean water level depth  $h_{MWL}$ , and wave gauge positions. Figure 3(a), on the whole wave gauges, appears that the present numerical  $H_s$  generally agree well with the experimental results with  $R^2$ , Skill, and MAPE values equal to 0.991, 0.998, and 3.402%. When comparing the predictions to other models at flat reef surface, such discrepancies may be primarily due to a complexity flow, shoaling phenomenon as the initial of stopping propagation waves, and wave

energy dissipation effects significantly. In addition, it could also be observed that  $H_s$  decreases rapidly in the flat reef caused by the breaking wave process.

Figure 3(b) depicts the present numerical  $h_{MWL}$  satisfactorily provide prediction results with  $R^2$ , Skill, and MAPE values equal to 0.980, 0.993, and 5.392%, respectively. Decreasing water depth could be fallen out in view of cross-fringing reef distribution between the slope reef area and the flat reef tip induced by shoaling before waves break. This suggests that unstable wave symmetry and mass conservation in NWT must be balanced by decreasing water depth in the reef edge. On the other hand, it revealed that wave propagation numerically along flat reef exposes the highest water depth. Therefore, the large magnitude of wave energy of flat reef has been reduced by breaking waves and bottom friction from itself. Overall, it seems that our prediction better captures the breaking wave height and breaking wave depth incident.

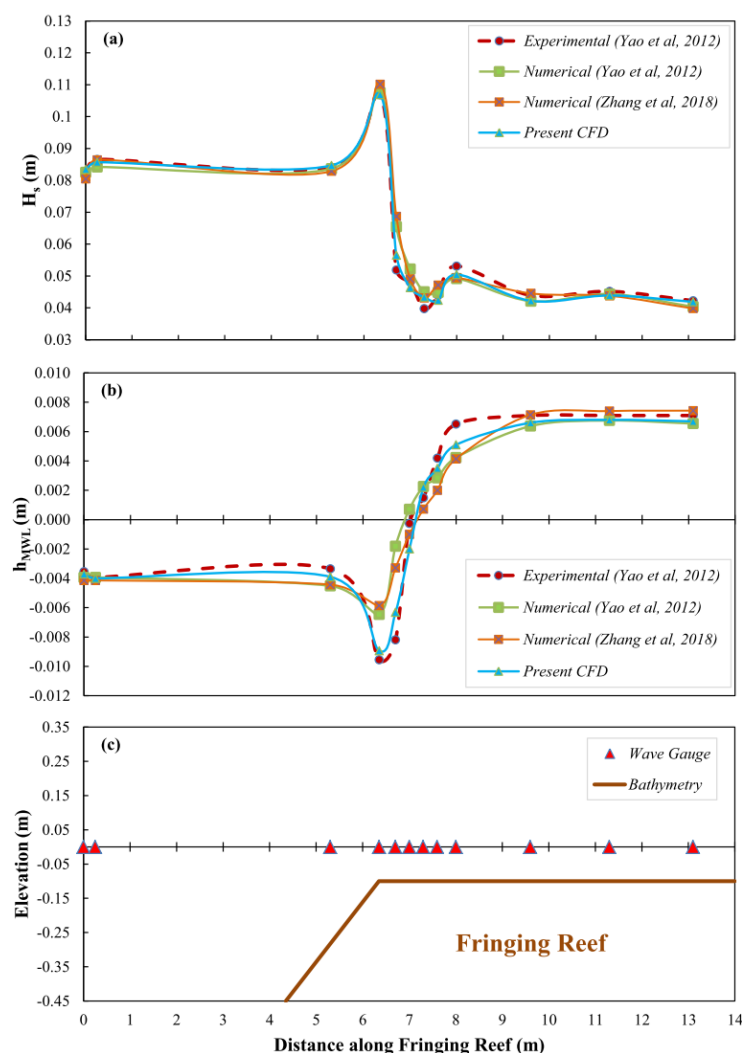


**Figure 3.** The numerical modelling validation, (a) Significant wave heights  $H_s$ , (b) Mean water level depth  $h_{MWL}$ , and (c) Wave gauge positions

### 3.2. Implementation of Breaking Wave Criteria Methods

#### 3.2.1. Locations of Relative Breaking Wave Height

Many criteria have been proposed to represent breaking wave on the fringing reef. However, most of these criteria only apply to constant water depth and gentle slopes. Consequently, [29] developed a

novel criterion method based on cases of breaking waves occurring on a steep slope, in both the slope reef and the flat reef are mentioned in equation (3) and (4), respectively.

The results using this method are illustrated in Figure 4, where the coefficient of determination  $R^2$  are 0.9018 and 0.9109, which could be said to be empirically and numerically related to the relative breaking wave height  $(H/h)_b$ . Based on these results, it is found that increasing the water depth at breaking wave location causes by decreasing  $(H/h)_b$ . If  $(H/h)_b$  decreases, the dependence of slope reef angle and the critical breaking wave height is relatively more dominant. As a complement to the final results of this method, it could be concluded that in the cases *B-1, C-1, D-1, B-2, C-2, D-2, B-3, C-3, D-3* included in the slope reef area. While the cases of *A-1, A-2, A-3, A-4, B-4, C-4, D-4* are in flat reef area.

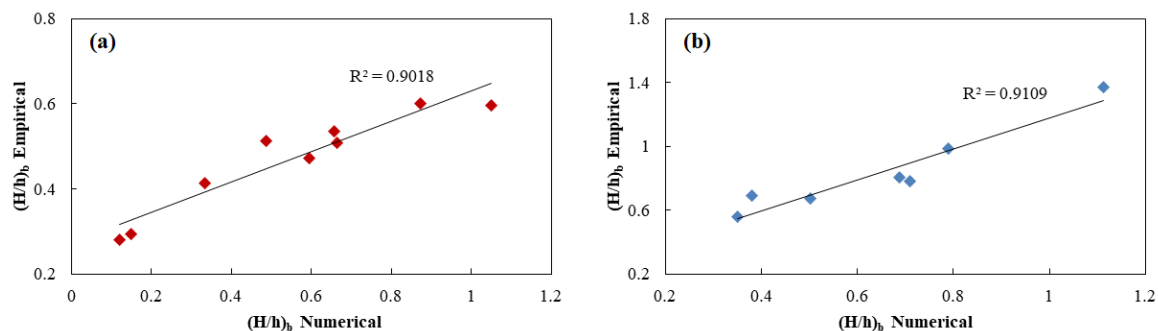


**Figure 4.** The coefficient of determination  $R^2$  between the numerical results and the empirical formula from Xu et al (2019), (a) Slope reef and (b) Flat reef

### 3.2.2. Estimation Ranges of Relative Breaking Wave Height

This second criterion method provides empirical constants with minimum and maximum values representing the lower and upper thresholds of breaking wave scatter data, respectively. In equation (5) proposed by [30] estimates the local maximum ratio of the relative breaking wave height parameter  $(H/h)_b$  for a certain wave period. The estimation range of these criterion is based on the grouping of water depth parameter  $h$ , so that it could be written as Group I (*A-1, B-1, C-1, D-1*), Group II (*A-2, B-2, C-2, D-2*), Group III (*A-3, B-3, C-3, D-3*), and Group IV (*A-4, B-4, C-4, D-4*).

In the Figure 5, there is an increasing of relative breaking wave height  $(H/h)_b$  causes by decreasing water depth of relative breaking wave  $h_b/gT_p^2$ . This is due to the higher  $(H/h)_b$  then shoaling effect is more visible and it could be occurred breaking wave quickly when minimum – maximum slope is to be gentler. Therefore, the energy dissipation increases drastically as the waves propagates along the flat reef. These criteria are divided into three categories, comprising qualify, overestimate, and underestimate. According to Figure 5(a) to 5(d), it could be concluded that the results obtained are quite well. In the qualifying category, there is only maximum two cases per group that match or in other words around 43.75% of breaking waves are in the qualify category. It is different with the overestimate category, the simulation of maximum estimated breaking waves is only 25% due to the tracking of wave propagation in NWT which is not stable in constant water depth. Most likely the equation (6) only applies to the cases of a gentle slope generally. On the other hand, the underestimate category obtained 31.25% of the minimum estimated breaking waves. It could be interpreted that the breaking wave height is relatively unbroken, and the whole wave asymmetry is stable well. From the three previous categories explanation, it could be assumed that several cases that meet the qualifying category are consist of *D-1, A-2, B-2, B-3, C-3, B-4, C-4*. Then, the overestimated category are in *A-1, C-2, D-2, D-4*. Finally, *B-1, C-1, A-3, D-3, A-4* are in the underestimated category.

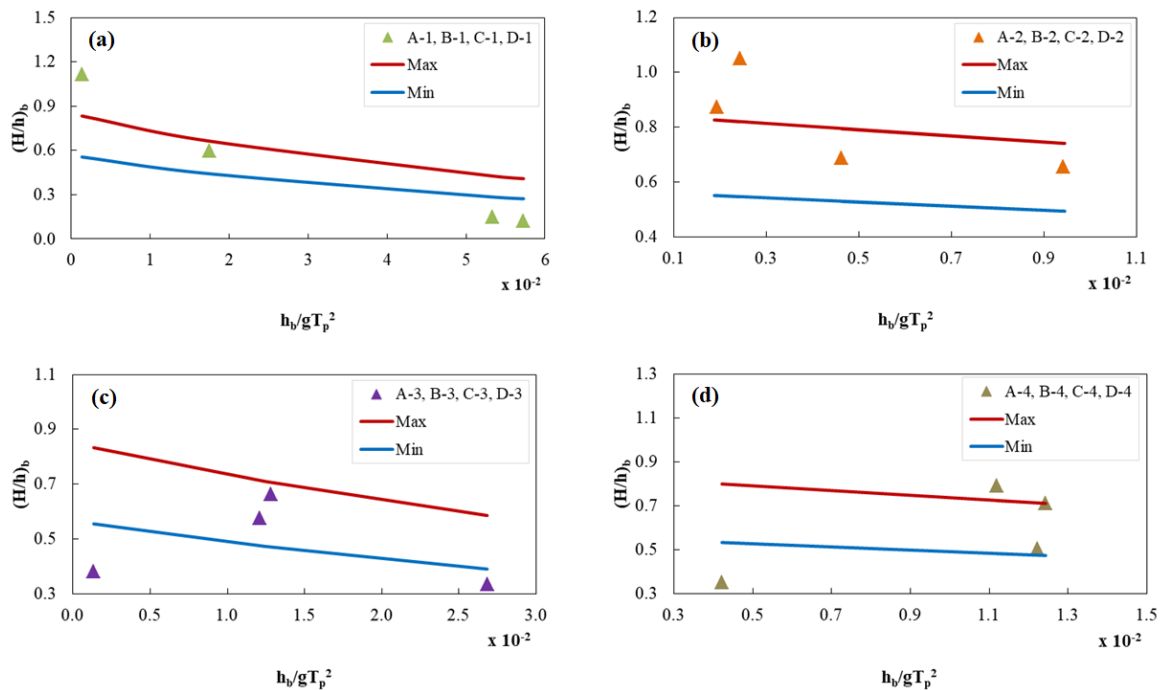


**Figure 5.** The breaking wave criteria according to Goda (2010) are in varying water depths  $h$ , (a) 0.364 m, (b) 0.378 m, (c) 0.392 m, and (d) 0.406 m

### 3.2.3. Probability of Breaking Wave

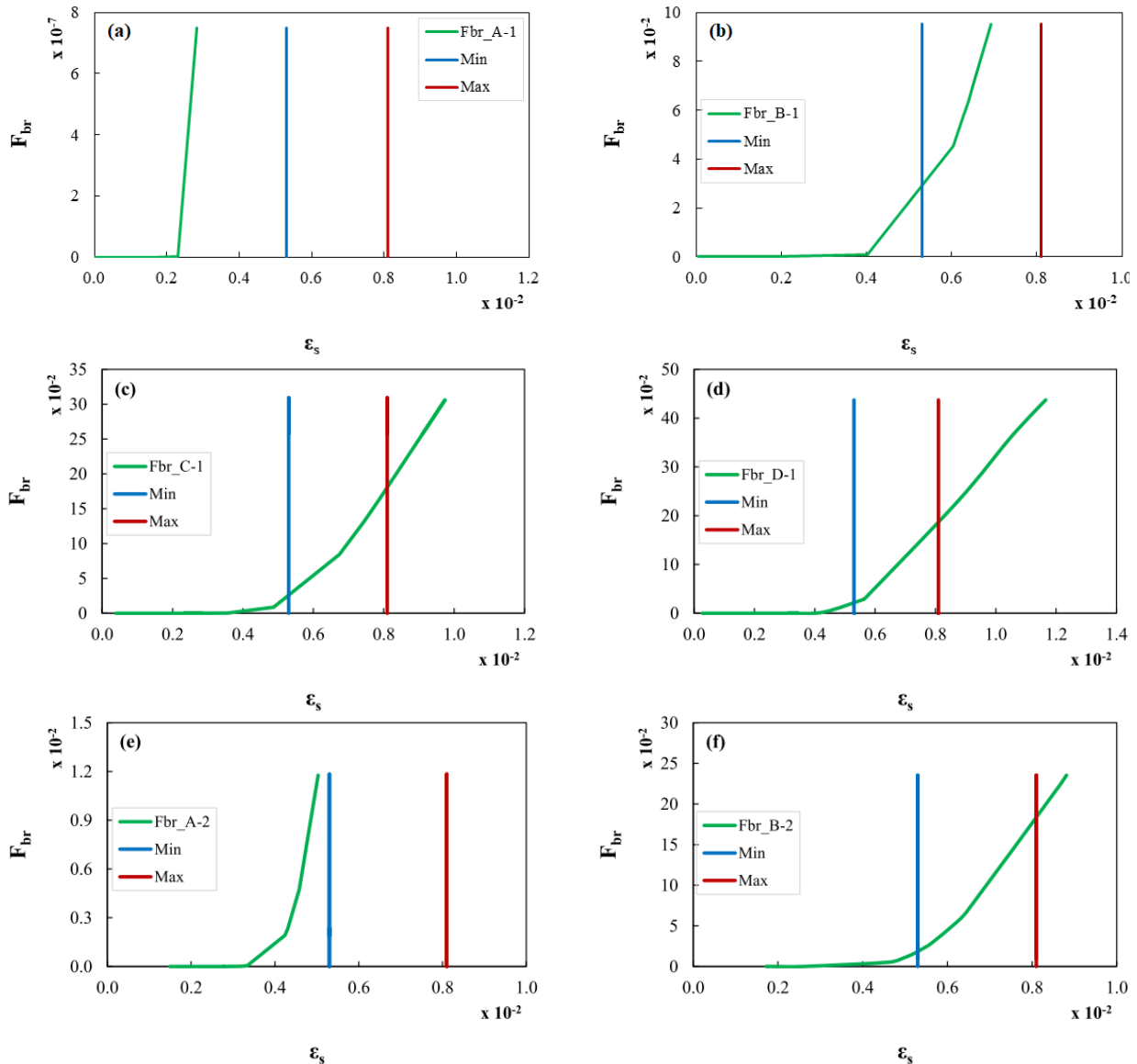
When the waves will break through the breaker point location periodically with varying velocity at temporal time, the possibility of breaking waves will change their position or unbreak. Therefore, [31] proposed the linear wave theory converting concept from temporal to spatial aspects in order to some precise estimates of breaking waves as indicated by equation (6) and (7), respectively. According this method, the breaking wave occurs when the wave crest acceleration is faster than the wave body acceleration itself. Nevertheless, this criterion focuses on the probability of breaking wave with respect to the significant wave steepness  $\varepsilon_s$ .

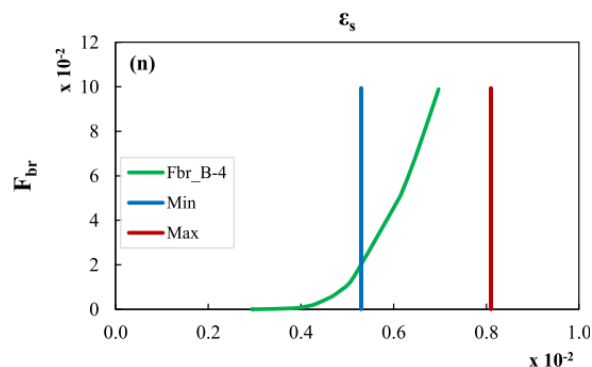
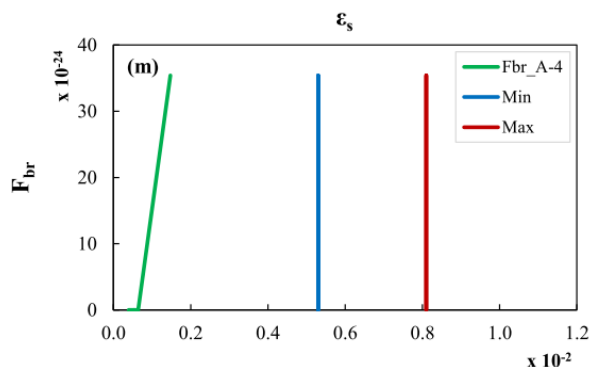
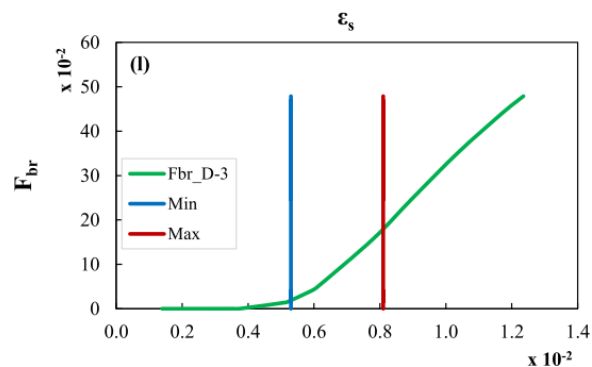
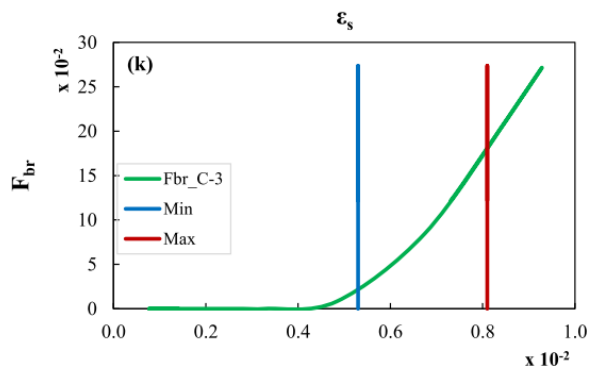
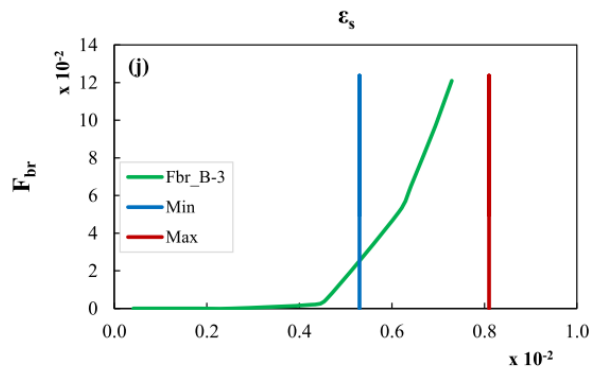
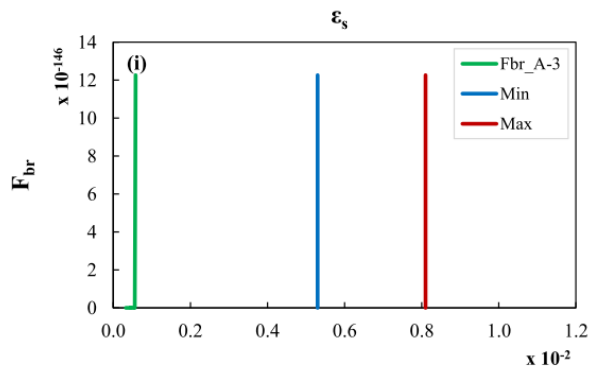
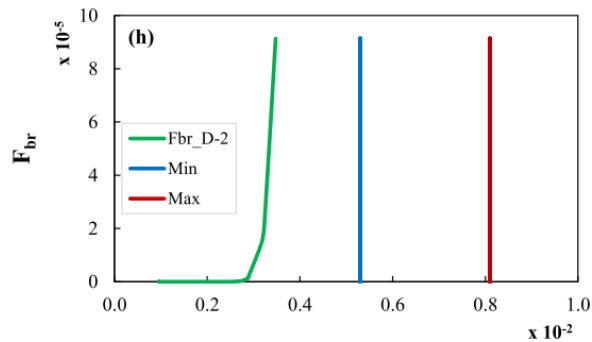
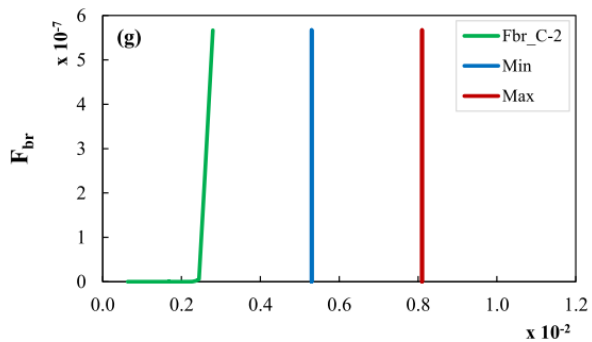
According to Figure 6, it is known as the  $\varepsilon_s$  increases significantly causes by increasing in the probability of breaking wave occurrence  $F_{br}$ . The parameters of the probability of breaking wave from total propagation waves are determined based on the intersection line between  $F_{br}$  and  $\varepsilon_s$  minimum as the smallest probability of occurrence. Then, the intersection line between  $F_{br}$  and  $\varepsilon_s$  maximum is as the largest probability of occurrence. Judging from the explanation, there are three possible events resulting from these parameters, comprising the probability obtained intersection lines from  $\varepsilon_s$  minimum to  $\varepsilon_s$  maximum is the first event, the second event is obtained from one of the  $\varepsilon_s$  minimum or  $\varepsilon_s$  maximum only, and the last event does not occur intersection line from  $\varepsilon_s$  minimum or  $\varepsilon_s$  maximum at all.

After identifying the three probability events from previous statement, the sequential case sets listed in Figure 6(a) to 6(p) could be verified in terms of the  $F_{br}$ . Some cases that fall into the first event consist of C-1, D-1, B-2, C-3, D-3, C-4 are attached in Figure 6(c-d-f-k-l-o). The results of intersection line of the probability from each wave propagation cases are converted into the number of breaking waves, comprising case of C-1= 1.080 – 8.820 times event, D-1= 1.030 – 8.840 times, B-2= 0.833 – 9.016 times, C-3= 0.990 – 8.145 times, D-3= 0.061 – 5.760 times, and C-4= 0.917 – 8.460 times. In summary, the wave slope, relative wave height, and relative water depth have a high impact on the first probability event. Meanwhile, the cases that fall into the second probability events are case of B-1= 1,380 times, B-3= 1,170 times, B-4= 1,092 times, and D-4= 8,460 times which are illustrated in Figure 6(b-j-n-p). The wave slope parameter is the main factor in this event. This result could be

seen carefully in each case there is only an intersection line, both minimum and maximum probabilities.

On the other hand, Figure 6(a-e-g-h-i-m), the third probability event includes cases of A-1, A-2, C-2, D-2, A-3, and A-4. It is no intersection line at all because the wave parameter simulation results have the wave slope, relative wave height, and relative water depth tends to be of small, so that the adoption of the two previous methods to the six cases of this third probability does not generate in breaking wave criteria.





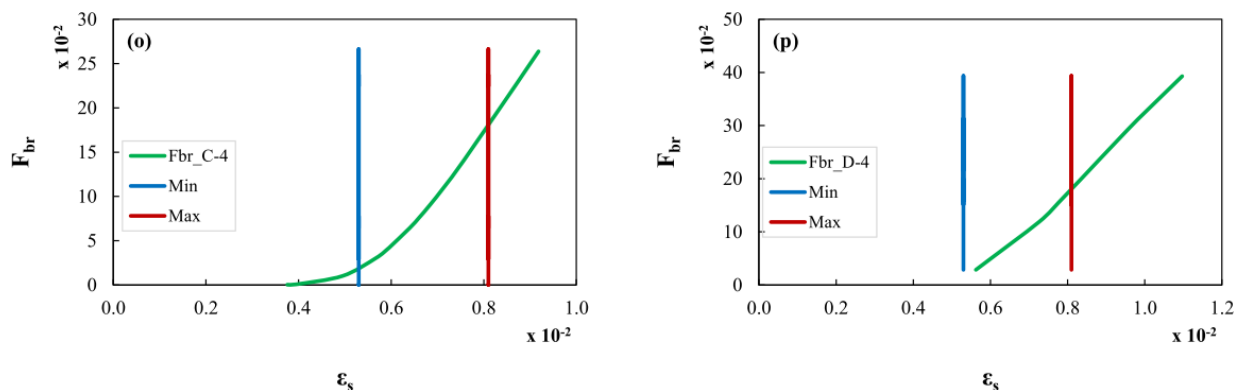


**Figure 6.** The breaking wave criteria according to Massel (2007) under various scenarios, (a) *A-1*, (b) *B-1*, (c) *C-1*, (d) *D-1*, (e) *A-2*, (f) *B-2*, (g) *C-2*, (h) *D-2*, (i) *A-3*, (j) *B-3*, (k) *C-3*, (l) *D-3*, (m) *A-4*, (n) *B-4*, (o) *C-4*, and (p) *D-4*. Green Lines - probability of breaking wave occurrence  $F_{br}$ ; blue lines – minimum significant wave steepness; red lines - maximum significant wave steepness

### 3.3. Impact Assessment for Positioning Wave Energy Converter

In this subsection, we apply the well-validated breaking wave criteria to examine the scenarios of the relative breaking wave height, the relative water depth, wave steepness, and probability of breaking wave occurrence that may affect the positioning wave energy converter (WEC). The lists of scenario that justify to be assessed in more impact detail are *D-1*, *B-2*, *C-3*, and *C-4*. The characteristics between the propagating wave height and wave nonlinearity from each wave gauge will be studied further as presented in Figure 7 and Figure 8, respectively. In order to understand the characteristics easily, the propagation of significant wave height  $H_{gauge}/H_i$  is compared with distance of each wave gauge on the NWT  $X_{gauge}/L_{NWT}$ .

The first well-validated scenario, *D-1*, illustrated in Figure 7(a), shows that the discrepancy of pre-breaking wave height is the smallest among others of 0.07. It induced by the slope angle of breaker point while the breaking waves are taking place in the slope reef area. The occurrence of small breaking wave height is due to the low water depth that means shoaling is quite small. Meanwhile, the degradation of propagating wave height of 0.64 taken place in post-breaking due to energy dissipation over water depth transformation. Second, Figure 7(b) is presented the breaker point *B-2* in the slope reef. When the wave propagates towards the fringing reef, the incident wave height stands apart post-breaking wave height of 0.21. In addition, it was found that decreasing wave height of 0.78 after the waves is in post-breaking. Moreover, the breaking wave *C-3*, illustrated in Figure 7(c), is similar to previous scenarios too. It was found that the pre-breaking wave height runs counter to 0.345 of the largest of all post-breaking. This is produced by sloping area of breaker point. Similar to the difference in pre-breaking, the degradation of the post-breaking wave height was the largest of all scenarios at 0.78 due to the significant energy dissipation. At the last moment, the breaking wave *C-4* occurs in flat reef area, shown in Figure 7(d). When the wave propagates towards the fringing reef, pre-breaking wave height differ 0.197 than average breaking wave height. It may be seen that decreasing post-breaking wave height is about 0.40.

In observing the fluid flow, the Froude number  $F_r$  is applied and to investigate the wave nonlinearity, Ursell number  $U_r$  is adopted. Based on Figure 8, it can be said that the Froude number of all selected scenarios generally falls into the subcritical flow category ( $F_r < 1$ ). All simulation results of each investigated scenario tend to be similar in terms of the increasing  $F_r$  from pre-breaking to breaking conditions. Therefore, the breaking wave celerity is very important to harnessing wave energy. When breaking condition leads to post-breaking, the  $F_r$  of *D-1*, *B-2*, and *C-3* scenario is steeper degradation than *C-4*. Another phenomenon that needs to be known is that the increasing celerity between pre-breaking and breaking was not included in the maximum value. In other words, the highest celerity taken place right after the post-breaking incident while the  $F_r$  converts to 0.52,

0.17, and 0.19. Only scenario *C-4* crops up the same celerity before and after the breaking event of 0.09. This is because the water depth effect on fringing reef  $h_r$  that greatly affects the breaking wave celerity. On the other hand, the  $U_r$  results from all scenarios satisfy in the shallow water ( $U_r > 15$ ) referring to Dawson (1981). Further, the  $U_r$  value of incident wave was less than thirty. It should be noted that scenario *D-1*, and *B-2* are obtained  $U_r$  greater than 100. This contradicts the  $U_r$  results of *C-3*, and *C-4* less than 100. This abnormality is highly depended on breaking wave height and breaking wave length, respectively. If the  $U_r$  is greater, the wave steepness and inconsistency wave geometry will also increase.

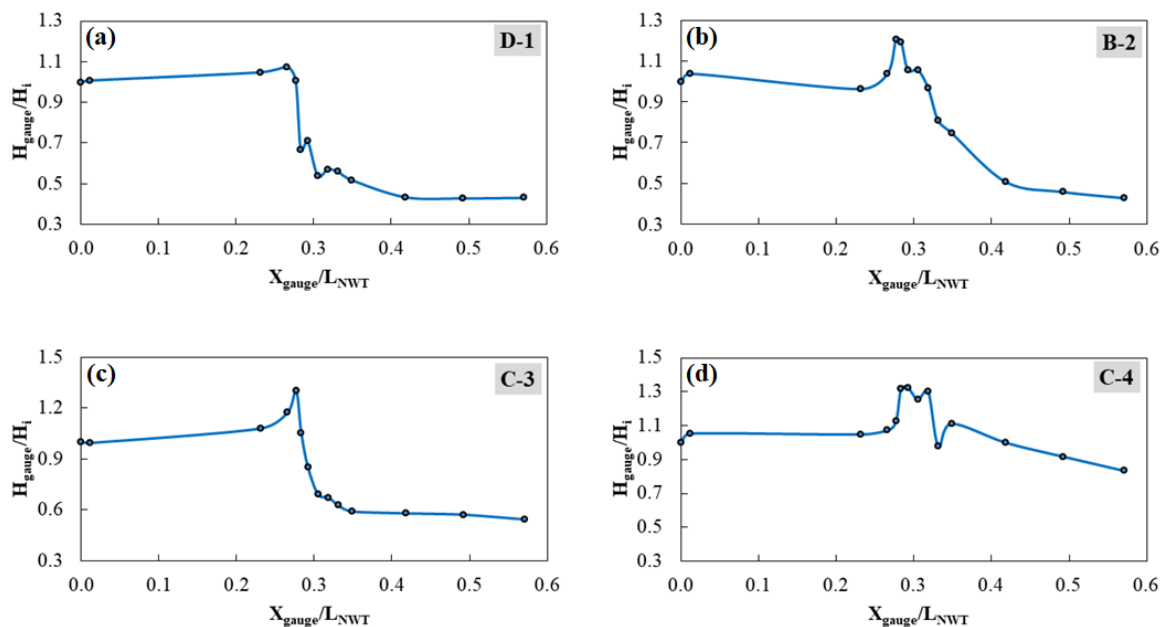


**Figure 7.** The transformations of wave propagation in each selected scenarios

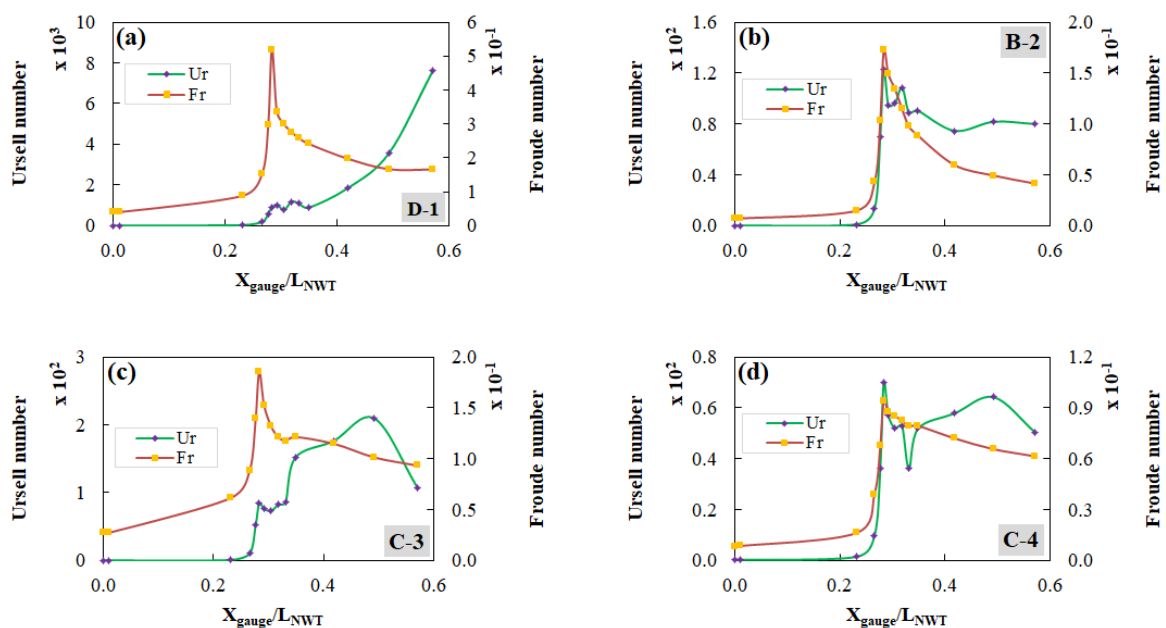


**Figure 8.** The Froude number  $F_r$  and Ursell number  $U_r$  in each selected scenarios

#### 4. Conclusion

The propagation of breaking waves over a fringing reef in NWT is investigated through LES modelling. The free surface is tracked by the VoF method. Three existing numerical and experimental studies with varying wave height, wave period, and water depth based on different breaking wave parameters are employed to validate the numerical model. The breaking waves are classified based on three common criteria available in literature. The investigations show that present CFD model outperforms the previously used numerical models in view of its capability to better emulate the breaking waves on the slope or flat reef else. The present model is then implemented to examine the impact assessments for positioning WEC. All common criteria are reasonably applicable to predict breaking wave incident. The results show that the four selected scenarios are most sensitive to the whole scenarios. These findings indicate that the energy dissipation occurs significantly during post-breaking wave height degradation such as *C-3*, *B-2*, *D-1*, and *C-4*, respectively. From pre-breaking to breaking conditions, celerity of breaking waves is expected to experience larger harnessing wave energy. Moreover, relative wave-breaker locations, relative wave-breaker height range, breaking wave probability, wave steepness, water depth, and slope fringing reef are induced by fluid flow and wave nonlinearity for generating violent breaking wave. Further studies could shed more light on the relationship between breaking wave force and WEC.

#### References

- [1] Roeber V and Cheung K F 2012 Boussinesq-type model for energetic breaking waves in fringing reef environments *Coast. Eng.* **70** 1–20
- [2] Lin P 2004 A numerical study of solitary wave interaction with rectangular obstacles *Coast.Eng.* **51** pp 35-51
- [3] Chella M A, Bihs H, Myrhaug D *et al* 2017 Breaking solitary waves and breaking wave forces on a vertically mounted slender cylinder over an impermeable sloping seabed *J. Ocean Eng.Mar. Energy* **3** pp 1–19
- [4] Zhang S, Zhu L, Li J 2018 Numerical simulation of wave propagation, breaking, and setup on steep fringing reefs *Water* **10** p 1147
- [5] Yao Y, Huang Z H, He W R and Monismith S G 2018 Wave-induced setup and wave-driven current over Quasi-2DH reef-lagoon-channel systems *Coast. Eng.* **138** pp 113–125
- [6] Yao Y, Zhang Q, Chen S and Tang Z 2019 Effects of reef morphology variations on wave processes over fringing reefs *Applied Ocean Research* **82** pp 52-62
- [7] Kamath A, Chella M A, Bihs H and Arntsen Ø A 2017 Energy transfer due to shoaling and decomposition of breaking and non-breaking waves over a submerged bar *Eng. Appl. Comput. Fluid Mech.* **11** pp 450–466
- [8] Lin P and Liu P L F 1998b Turbulence transport, vorticity dynamics, and solute mixing under plunging breaking waves in surf zone *J. Geophys. Res.* 103 pp 15677–15694
- [9] Lin P, Chang K A and Liu P L F 1999 Runup and rundown of solitary waves on sloping beaches *ASCE J. Waterw. Port Coast. Ocean Eng.* 125 pp 247–255
- [10] Fang K, Zou Z, Dong P, Liu Z, Gui Q and Yin J 2013 An efficient shock capturing algorithm to the extended boussinesq wave equations *Appl. Ocean Res.* 43 pp 11–20
- [11] Wei Z and Dalrymple R A 2018 Surf zone wave heating by energy dissipation of breaking waves *Coastal Engineering Proceedings* 1 p 2
- [12] Lowe R J, Buckley M, Altomare C, Rijnsdorp D *et al.* 2019 Numerical simulations of surf zone wave dynamics using Smoothed Particle Hydrodynamics *Ocean Modelling* **144** p 101481
- [13] Darvishi E, Fenton J D and Kouchakzadeh S 2016 Boussinesq equations for flows over steep slopes and structures *J. Hydraul. Res.* 55 pp 324–337
- [14] Yao Y, He T, Deng Z, Chen L and Guo H 2019 Large eddy simulation modeling of tsunami-like solitary wave processes over fringing reefs *Nat. Hazards Earth Syst. Sci.* pp 1281–1295.
- [15] Lubin P, Vincent S, Caltagirone J and Abadie S 2003 Fully three-dimensional numerical simulation of a plunging breaker *C. R. M´ecanique* 331 pp 495–501

- [16] Yao Y, Huang Z, Stephen G, Monismith, Edmond Y M 2012 1DH Boussinesq modeling of wave transformation over fringing reefs *Ocean Engineering* pp 30-42.
- [17] Davidson, J. dan Costello, R. (2020), "Efficient Nonlinear Hydrodynamic Models for Wave Energy Converter Design—A Scoping Study", *Journal of Marine Science and Engineering*, Vol. 8, hal. 35.
- [18] Zhiyin, Y. (2015), "Large Eddy Simulation: Past, Present and the Future", *Chinese Journal of Aeronautics*, Vol. 28, hal. 11-24.
- [19] Melville, W.K. (1982), "The Instability and Breaking of Deepwater Waves", *Journal of Fluid Mechanics*, Vol. 722, hal. 165–185.
- [20] Windt, C., Davidson, J., Schmitt, P. dan Ringwood, J.V. (2019), "On the Assessment of Numerical Wave Makers in CFD Simulations", *Journal of Marine Science and Engineering*, Vol. 7, hal. 47.
- [21] Fernandes, A. M. dan Fonseca, N. (2013), "Finite Depth Effects on the Wave Energy Resource and The Energy Captured by a Point Absorber", *Ocean Engineering*, Vol. 67, hal. 13-26.
- [22] DNV-RP-C205 (2010), Recommended Practice: Environmental Conditions and Environmental Loads, Det Norske Veritas, Norway.
- [23] CEM EM-1110-2-1100 (2015), Coastal Engineering Manual part II, US Army Corps of Engineers, Washington DC.
- [24] Schmitt, P. dan Elsaesser, B. (2015), "A Review of Wave Makers for 3D Numerical Simulations", *Proceedings of the MARINE 2015—Computational Methods in Marine Engineering VI*, Rome, hal. 437–446.
- [25] Aggarwal, A., Alagan Chella, M., Bihs, H., dan Myrhaug, D. (2020), "Properties of Breaking Irregular Waves over Slopes". *Ocean Engineering*, hal 216.
- [26] Gomes, A., Pinho, J.L.S., Valente, T., Antunes do Carmo, J.S.V. dan Hegde, A. (2020), "Performance Assessment of a Semi-Circular Breakwater through CFD Modelling", *Journal of Marine Science and Engineering*, Vol. 8, hal. 226.
- [27] Willmott, C. J. (1981), "On the Validation of Models", *Physics and Geography*, Vol. 2, hal. 184–194.
- [28] Myttenaere, A., Golden, B., Grand, B. Le. dan Rossi, F. (2016), "Mean Absolute Percentage Error for Regression Models", *Neurocomputing*, Vol. 192, hal. 38–48.
- [29] Xu, J., Liu, S., dan Li, J. (2019), "Experimental Study of Wave Propagation Characteristics on a Simplified Coral Reef", *Journal of Hydrodynamics*, Vol. 32, hal. 385–397.
- [30] Goda, Y. (2010), "Reanalysis of Regular and Random Breaking Wave Statistics", *Coastal Engineering Journal*, Vol. 52, hal. 71–106.
- [31] Massel, S.R. (2007), "Ocean Waves Breaking and Marine Aerosol Fluxes: Wave Breaking Criteria and Probability of Breaking", *Atmospheric and Oceanographic Sciences Library*, Springer, New York.
- [32] Kench, P. S. dan Mann, T. (2017), "Reef Island Evolution and Dynamics: Insights from the Indian and Pacific Oceans and Perspectives for the Spermonde Archipelago", *Frontier on Marine Science*, Vol. 4, hal. 145.
- [33] EMEC (2009), *Marine Renewable Energy Guides : Tank Testing of Wave Energy Conversion Systems*, The European Marine Energy Centre, London.
- [34] Payne, G. (2008), *Guidance for the Experimental Tank Testing of Wave Energy Converters: version 01b*, Super Gen Marine, University of Edinburgh, Edinburgh.